Geomechanics and Engineering, *Vol. 18, No. 4 (2019) 373-389*
DOI: https://doi.org/10.12989/gae.2019.18.4.373

Prediction model of service life for tunnel structures in carbonation environments by genetic programming

Wei Gao* and Dongliang Chen[a]

Key Laboratory of Ministry of Education for Geomechanics and Embankment Engineering, College of Civil and Transportation Engineering, Hohai University, Nanjing 210098, PR China

(Received January 3, 2019, Revised June 20, 2019, Accepted June 23, 2019)

Abstract. It is important to study the problem of durability for tunnel structures. As a main influence on the durability of tunnel structures, carbonation-induced corrosion is studied. For the complicated environment of tunnel structures, based on the data samples from real engineering examples, the intelligent method (genetic programming) is used to construct the service life prediction model of tunnel structures. Based on the model, the prediction of service life for tunnel structures in carbonation environments is studied. Using the data samples from some tunnel engineering examples in China under carbonation environment, the proposed method is verified. In addition, the performance of the proposed prediction model is compared with that of the artificial neural network method. Finally, the effect of two main controlling parameters, the population size and sample size, on the performance of the prediction model by genetic programming is analyzed in detail.

Keywords: prediction model; tunnel structure; genetic programming; service life; carbonation

1. Introduction

All structures are associated with problems of durability and service life from the day when they are built. Because underground structures are exposed to more complicated corrosion environments than other structures (Do *et al*. 2018, Sun 2011, Zeng *et al*. 2011, Zhang *et al*. 2017), it is important to study the problem of durability for underground structures. Due to their complexity, there are relatively few studies on the durability problems of underground structures, and they only were begun several years ago. However, the main structure of the tunnel is the lining structure, which is a typical reinforced concrete structure. Currently, the generally used methods to study reinforced concrete structures are applied to analyze the durability of tunnel structures (Do *et al*. 2014, Gokce *et al*. 2009, Miranda *et al*. 2015, Yuan *et al*. 2012, Spyridis 2014, Sun 2011). Generally, a reinforced concrete structure is corroded by two main factors: (i) carbonation and (ii) chloride-induced corrosion. Carbonation-induced corrosion most commonly occurs in relatively dry environments, where sufficient carbon dioxide to diffuse into the cover concrete is possible. As an example, the carbonation-induced corrosion for the tunnel structure is studied here.

It is very important to know that when structural damage due to reinforcement corrosion becomes visible, deterioration is usually at a late stage, and it may be too late to take any preventive or protection measures. Therefore, the service life prediction based on the corrosion damage of the structure is particularly important.

To estimate the corrosion damage of a reinforced concrete structure in a carbonation environment, there are two main methods: the theoretical method and the empirical method. For the theoretical method, based on the carbonation mechanism, the analytical model can be obtained using the diffusion law. For the empirical method, based on the results of the carbonation experiment, one analytical model can be obtained to fit the experimental data. Based on these two methods, there are an extensive variety of carbonation models (Ahmad 2003, Pan 2005, Taffese and Sistonen 2013, Woyciechowski and Soko 2017). However, this type of carbonation model cannot consider the complicated engineering uncertainty factors and require some assumptions to be constructed (Taffese and Sistonen 2017). Thus, it is difficult to predict the service life of reinforced concrete structures in carbonation environments for real engineering using those carbonation models. To solve this difficult problem, currently, artificial intelligent methods based on data analysis are used to forecast the service life of reinforced concrete structures with carbonation corrosion (Taffese and Sistonen 2017). For example, based on laboratory data, the artificial neural network is used to predict the carbonation depth of concrete (Akpinar and Uwanuakwa 2016, Kellouche *et al*. 2017, Lu and Liu 2009, Taffese and Al-Neshawy *et al*. 2015). To improve the traditional artificial neural network, new artificial neural networks based on the particle swarm optimization or the differential evolution algorithm are also used (Bu *et al*. 2009, Luo *et al*. 2014). Similarly, the support vector machine is applied to predict the carbonation depth of concrete (Xiang 2009). Moreover, the decision-tree-based learning algorithm is used to predict the carbonation depth of concrete (Taffese and Sistonen *et al*. 2015). However, these studies analyzed the carbonation of the

*Corresponding author, Professor
E-mail: wgaowh@163.com
[a]M.Sc.

http://www.techno-press.org/?journal=gae&subpage=7
ISSN: 2005-307X (Print), 2092-6219 (Online)

concrete and using the data from the laboratory tests. Thus, they cannot be used for reinforced concrete structures and cannot consider the real engineering factors. Recently, the artificial neural network has been used to predict the carbonation depth of reinforced concrete structures based on field data, and this type of studies can consider complicated engineering factors (Jesus *et al*. 2017). However, the prediction of the carbonation service life for underground structures based on the data analysis was not examined in the previous studies. Therefore, in this study, based on the data of real engineering conditions for real engineering examples, genetic programming is used to predict the carbonation service life of tunnel structures. Then, the explicit expression of the carbonation service life for tunnel structures can be obtained. Thus, this prediction model of the carbonation service life for tunnel structures by genetic programming can be easily popularized in real tunnel engineering.

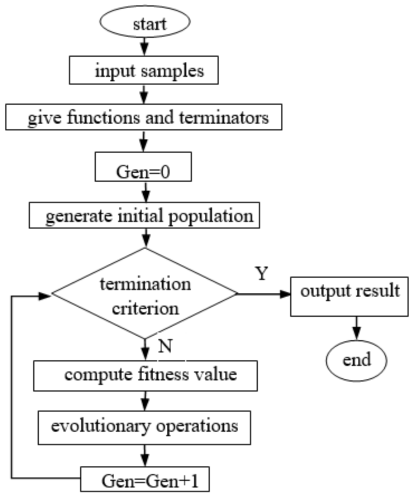

Fig. 1 Flow chart of GP

2. Brief introduction to genetic programming

Genetic programming (GP) is an evolutionary computing method to automatically generate computer programming, which was firstly proposed by American scholar Koza in the 1990s (Koza 1992). Its essence is to construct a mathematical model to describe the engineering phenomenon. Thus, GP is a good pattern recognition method in many fields such as automatic control, game strategy, symbolic regression, and empirical equation construction (Gao and Yin 2011, Ventura 2012).

The basic flow chart of GP is shown in Fig. 1.

The main operations of GP are as follows:

(1) Individual representation

The representation of an individual is a layering structure tree, as shown in Fig. 2. The expression described by the layering structure tree is also shown in Fig. 2.

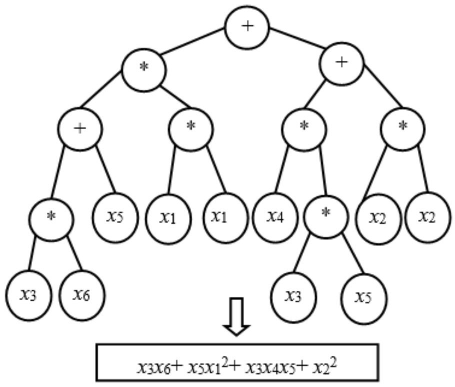

Fig. 2 Individual representation of GP

(2) Fitness function

The fitness function of an individual is generally a type of transformation of its objective function. In this study, the fitness function is described as

$$F = \frac{1}{1 + \sum_{i=1}^{n} (T_{ri} - T_{ci})^2} \tag{1}$$

where T_{ri} and T_{ci} are the real and computed life values, respectively; n is the number of samples.

(3) Evolutionary operators

a) Reproduction operator

There are two steps in this operator. First, an individual in the current generation is selected according to the reproduction probability. Second, this individual is directly copied to create an individual used in the next generation.

b) Crossover operator

Using the crossover operator, two new individuals are generated by exchanging some parts of two old individuals. The process of the crossover operator is shown in Fig. 3.

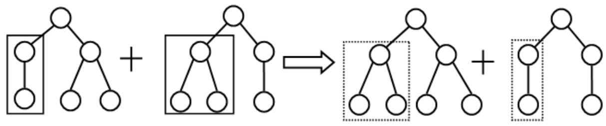

Fig. 3 Sketch map of the crossover operator

c) Mutation operator

Using this operator, one new individual is generated by changing some parts of the old individual. The process of the mutation operator is shown in Fig. 4.

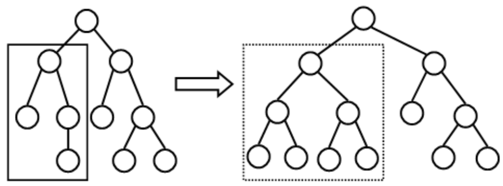

Fig. 4 Sketch map of the mutation operator

(4) Selection operation

Generally, the roulette wheel selection is used. For this operation, the selection probability of an individual is (Gao and Yin 2011, Koza 1992)

$$P = \frac{f_i}{\sum_{i=1}^{M} f_i} \tag{2}$$

where f_i is the fitness value of individual i; M is the number of individuals in the group.

(5) Termination criterion

Table 1 Tunnel engineering examples in China in a carbonation environment

Number	Average temperature	Relative humidity	CO_2 concentration	Rock mass grading	Burial depth	Clear width	Lining thickness
	T / °C	RH	C_0	Q	D / m	W / m	L / cm
1	21.8	0.78	0.0633	III	842	10.38	35
2	24	0.75	0.0532	IV	760	9.25	50
3	22.5	0.76	0.0538	III	1000	11.2	40
4	20.8	0.67	0.0653	IV	450	7.5	40
5	18.67	0.84	0.1452	V	643	9.5	50
6	21.8	0.78	0.0673	IV	98	20.7	45
7	12.5	0.48	0.0522	VI	65	14.82	60
8	11.7	0.53	0.0738	V	295	13.2	55
9	2	0.54	0.0655	V	1050	7.8	30
10	1.2	0.57	0.048	V	240	12.4	50
11	16	0.65	0.0972	IV	39	10.75	50
12	17.8	0.81	0.082	V	30	12.42	40
13	22	0.85	0.048	IV	14	15	65
14	11.2	0.49	0.0442	V	240	10.5	45
15	22	0.8	0.058	V	11	6.2	35
16	17	0.78	0.0432	IV	660	11.4	40
17	0.3	0.5	0.0425	VI	266	7.5	45
18	15.3	0.75	0.187	VI	51	14.5	60
19	17.5	0.78	0.065	IV	90	3.75	40
20	17.8	0.8	0.044	III	180	10.5	35
21	3.5	0.56	0.065	IV	995	9	35
22	21	0.83	0.064	V	1506	9	40
23	21.7	0.78	0.047	V	26.85	7.37	45
24	22	0.79	0.072	IV	28.1	7.5	40
25	18.1	0.8	0.053	III	47	12.5	35
26	22.93	0.83	0.0926	IV	87.6	10.5	40
27	16.7	0.68	0.134	IV	1270	12.5	40
28	16.2	0.7	0.077	V	477	12.86	40
29	15.2	0.54	0.071	IV	451.61	10.25	35
30	13	0.72	0.057	V	700	11.2	40
31	14.5	0.79	0.073	IV	545.2	7.8	50
32	15.4	0.57	0.078	V	445	5.4	35
33	21	0.77	0.081	IV	910	10.5	40
34	22	0.79	0.077	III	745	6.5	35
35	18.3	0.78	1.022	III	344	9.75	35
36	0.4	0.52	0.086	IV	277	7.5	40

Number	Cover thickness	Carbonation remains	Water-cement ratio	Lining strength	Design speed	Life	Area
	c / mm	x / mm	W/C	f / MPa	V / km/h	T_{ri} / $year$	
1	50	20.639	0.4	35	60	61.49	Xiamen
2	55	20.104	0.42	30	60	66.51	Chongqing
3	55	20.077	0.4	30	80	53.49	Guizhou
4	50	19.481	0.48	32.6	160	36.81	Shanxo
5	62	16.091	0.4	32.42	80	35.53	Dazhou

Table 1 Continued

Number	Cover thickness c / mm	Carbonation remains x / mm	Water-cement ratio W/C	Lining strength f / MPa	Design speed V / km/h	Life T_{ri} / year	Area
6	50	19.855	0.56	22.5	100	43.80	Guangzhou
7	65	15.279	0.48	31.5	200	93.87	Lanzhou
8	60	18.968	0.52	30	200	40.63	Dingxi
9	40	16.859	0.55	40	160	67.43	Wuwei
10	60	26.445	0.46	34.3	80	231.88	Qinghai
11	60	20.171	0.5	30	80	53.17	Anhui
12	50	18.127	0.5	30	160	52.85	Sichuan
13	50	16.836	0.32	50	80	37.40	Shanghai
14	55	18.623	0.4	16.7	60	48.01	Lanzhou
15	50	17.817	0.5	23.5	80	53.11	Shanghai
16	50	17.981	0.5	20	120	54.34	Yunnan
17	50	18.727	0.33	35	60	192.78	Qinghai
18	50	23.231	0.28	38.5	80	50.21	Nanjing
19	50	18.452	0.44	32	30	51.52	Ganzi
20	50	19.123	0.5	24	60	56.08	Sichuan
21	50	18.400	0.46	30	40	59.67	Xizang
22	50	20.848	0.48	26.7	30	32.91	Ya'an
23	50	19.639	0.42	35	250	77.34	Guiyang
24	60	21.557	0.43	32	250	57.96	Guangxi
25	45	17.601	0.42	28.7	70	43.58	Wenzhou
26	50	19.462	0.39	31.2	70	44.33	Xianggang
27	50	18.951	0.5	27.6	80	41.89	Shanaxi
28	50	17.173	0.48	28.4	80	42.88	Tianshui
29	45	17.643	0.46	30	80	41.30	Shanxi
30	45	18.238	0.5	27.8	70	39.28	Ankang
31	55	21.750	0.46	32.4	80	46.56	Anhui
32	45	16.233	0.4	34.3	160	48.56	Shanxi
33	50	18.215	0.42	28.5	100	79.40	Guangdong
34	50	15.794	0.4	28	100	63.35	Guangxi
35	45	14.382	0.42	32	80	88.40	Hunan
36	50	15.831	0.33	33.6	70	217.91	Yushu

The termination criterion specifies that the difference between the maximum fitness value and the average fitness value of a group is less than error ε. To avoid infinite iteration, a maximum number for evolutionary generations is provided.

Moreover, some parameters must be determined: the number of individuals, crossover probability, mutation probability, reproduction probability, ε and maximum number for evolutionary generations. Generally, these parameters are determined based on experience and a test.

3. Carbonation prediction model of a tunnel structure based on GP

For the tunnel environment, the inner side of the lining structure is exposed in the semiclosed air environment. In this space, air ventilation is difficult, and the relative temperature difference between inside and outside is small. Therefore, the CO_2 concentration in the tunnel will increase to five times of that in air with the aggregation of the automobile exhaust (Feng and Tian 2014, Sun 2011). In this environment, the corrosion of the lining concrete structure caused by penetration of CO_2 is a decisive factor for reducing the service life of the tunnel structure.

According to previous studies (Pan 2005, Ranjith *et al.* 2016), the main mechanism of CO_2 corrosion to the tunnel structure is as follows. CO_2 transports and diffuses from the inner side of the lining to the interior of the lining structure and chemically reacts with the alkaline hydration substance to create carbonate or other substances. Thus, the alkaline environment of the lining structure will be destroyed. When the PH value is less than 8.5, the steel passivation film will disappear. Then, the steel will rust because of oxygen gas and water. Due to the expansive force caused by the steel rusting, the lining structure will crack and break. Thus, the service life of the tunnel structure will decrease. Moreover, the lining structure will become brittle by CO_2, and its ductility will be reduced. Thus, the service life of the tunnel structure will also decrease.

Based on the main carbonation mechanism and previous studies (Feng and Tian 2014, Sun 2011, Yuan *et al*. 2012), the main factors to affect the carbonation service life of a tunnel structure are: the design CO_2 concentration in the tunnel of the tunnel engineering (C_0), average annual temperature of the tunnel engineering (T), average annual relative humidity of the tunnel engineering (RH), water-cement ratio of the tunnel structure (W/C), compressive strength of the lining structure (f), thickness of the concrete cover for the structure (c), burial depth of the tunnel (D), rock mass grading of the tunnel engineering (Q), clear width of the tunnel inner diameter (W), lining thickness of the tunnel engineering (L), carbonation remains of the lining cement (x), and design speed of the tunnel engineering (V).

To construct the carbonation prediction model of the tunnel structure, typical engineering examples were collected as data samples. In this study, 36 tunnel engineering examples in China in carbonation environments were applied, as shown in Table 1. Because the main factors to affect the carbonation service life considered here are numerous, the complete data for 36 engineering examples cannot be found in one reference. Even for one engineering example, its complete data may not be found in one reference too. Thus, according to the main factors, the complete data for 36 engineering examples were collected from many references, as shown in the Appendix.

3.1 Verification of the new prediction method

3.1.1 Carbonation prediction model with two influential factors

To verify the method of the construction prediction model using GP, first, a simple model considering two influence factors, which are the concrete cover thickness (c) and water-cement ratio (W/C), is analyzed.

In this study, the function set is $F=\{+,-,\times,\div,\mathrm{power},\ln,\exp,\sin,\cos\}$, and the terminator set is $M=\{c,\frac{W}{C}\}$. The 20 data samples used in this study are shown in Table 2, which are imported from Table 1. The first 15 samples in Table 2 are used to construct the model and are called training samples, and the last 5 are used to verify the constructed model and called testing samples. The typical carbonation model for reinforced concrete structures proposed by Kishitani (Pan 2005) is used to compute the life of the tunnel structure. This model can be described as

$$t=\frac{c^2\times[0.3(1.15+3\frac{W}{C})]}{(r_c r_a r_s)^2\times(\frac{W}{C}-0.25)^2}\quad \text{if}\quad \frac{W}{C}\geq 0.6 \tag{3}$$

Table 2 Data samples to construct the carbonation prediction model with two factors

Number	Cover thickness c / mm	Water-cement ratio W/C	Life T_{ri} / year
1	50	0.4	83.14
2	55	0.42	91.31
3	55	0.4	103.52
4	50	0.48	40.68
5	62	0.4	131.54
6	50	0.56	26.45
7	65	0.48	69.02
8	60	0.52	38.14
9	40	0.55	21.40
10	60	0.46	73.15
11	60	0.5	47.12
12	50	0.5	37.18
13	50	0.32	232.31
14	55	0.46	66.76
15	45	0.4	63.90
16	50	0.42	79.31
17	45	0.42	56.23
18	60	0.33	283.17
19	50	0.38	91.31
20	60	0.43	103.52

$$t=\frac{7.2c^2}{(r_c r_a r_s)^2\times(4.6\frac{W}{C}-1.76)^2}\quad \text{if}\quad \frac{W}{C}<0.6 \tag{4}$$

where t is the life, c is the concrete cover thickness, W/C is the water-cement ratio, r_c is the influence coefficient of concrete admixtures, r_a is the influence coefficient of aggregate types, and r_s is the influence coefficient of cement types. It must be noted that, the three coefficients are different for different engineering, and are determined according to the real engineering conditions. Here, they can be determined as follows: r_c=0.968+0.032CA, where CA is the amount of the concrete admixtures; r_a are 1 for the ordinary sand, 1.4 for the broken light sand, and 2 for the perlite sand; r_s are 1 for ordinary Portland cement, 1.43 for slag Portland cement, 1.56 for fly-ash Portland cement, and 1.78 for fly-ash slag Portland cement.

The results are as shown in Table 2. In this study, the computed life by the empirical model shown in functions (3)-(4) is presented as the real life. Based on experience (Gao and Yin 2011, Koza 1992) and our test, the main parameters of GP are determined as follows: the number of individuals is 40; the crossover probability is 0.9; the mutation probability is 0.05; the reproduction probability is 0.1; ε is 10^{-5}; the maximum number for evolutionary generations is 100.

The data of the training samples in Table 2 are used in the GP programmed by MATLAB, and the prediction model considering two factors can be obtained as

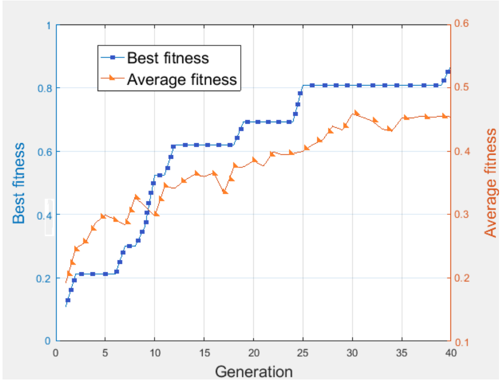

Fig. 5 Evolutionary process of the best fitness and average fitness for the carbonation prediction model with two factors

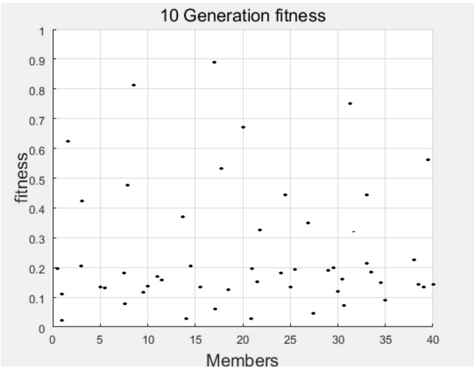

(a) 10 evolutionary generations

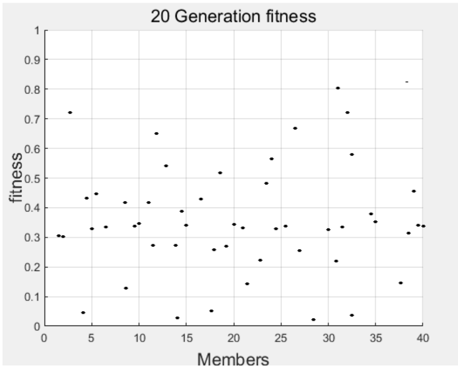

(b) 20 evolutionary generations

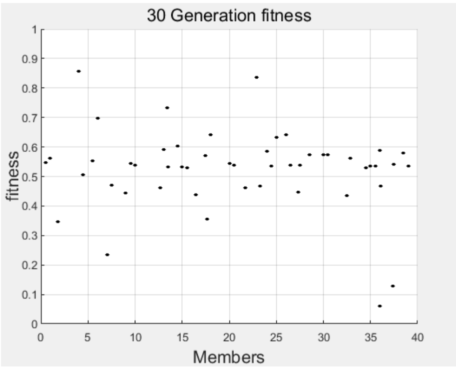

(c) 30 evolutionary generations

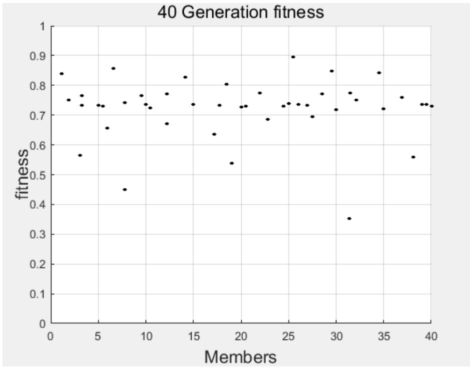

(d) 40 evolutionary generations

Fig. 6 Distribution of individual fitness for the carbonation prediction model with two factors

$$t = 0.1 \times \left(\frac{c}{12.1\frac{W}{C} - 3.2} \right)^2 \tag{5}$$

where t is the life, c is the concrete cover thickness, and W/C is the water-cement ratio.

The evolutionary process of the best fitness and average fitness of one group is shown in Fig. 5. The distributions of individuals in the evolutionary process are shown in Fig. 6.

Fig. 5 shows that with the increase of the number for evolutionary generations, all values of best fitness and average fitness gradually improve and tend to remain at one specific value, especially for the average fitness. Hence, when the computing process continues, the fitness values increase to a stable one. In other words, the algorithm converges. Moreover, the best fitness is the fitness value of the best individual in the population. The best individual in the population may be same for several generations. When some generations have past, the new best individual can be found. Therefore, the sudden rise can be observed on the best fitness curve. Fig. 6 shows that as the evolutionary generation increases, the individual fitness in the population is gradually congregated. In other words, the discreteness of individual fitness in the population is gradually decreased. Therefore, as shown in Figs. 5 and 6, the searching process of GP converges, and the performance of GP is satisfactory.

Using the constructed model by GP, the computed lives of tunnel structures for training samples are summarized in Table 3.

From Table 3, for 15 training samples, the computing results by new carbonation prediction model are consistent with the real lives. The average relative error is only 0.16.

To verify the constructed model, the model was used to compute the lives of 5 testing samples. The results are

Table 3 Computing results for the training samples by the carbonation prediction model with two factors

Number	Real life	Computing life	Absolute error	Relative error
1	83.14	92.95	9.82	0.1181
2	91.31	85.41	5.90	0.0646
3	103.52	112.47	8.95	0.0865
4	40.68	36.76	3.92	0.0964
5	131.54	142.92	11.38	0.0865
6	26.45	19.55	6.90	0.2609
7	69.02	62.12	6.90	0.1000
8	38.14	37.66	0.48	0.0126
9	21.40	13.40	8.00	0.3738
10	73.15	65.97	7.18	0.0981
11	47.12	44.32	2.8	0.0594
12	37.18	30.78	6.4	0.1721
13	232.31	353.61	121.30	0.5221
14	66.76	55.43	11.33	0.1697
15	63.90	75.29	11.39	0.178
Average value	—	—	14.84	0.16

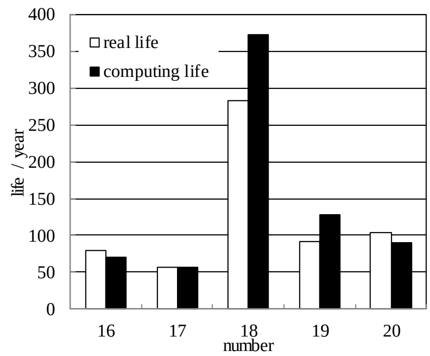

Fig. 7 Computing results of the testing samples by the carbonation prediction model with two factors

shown in Fig. 7.

In Fig. 7, all differences between the predicted lives by the constructed model and the real lives for 5 testing samples are small, except for sample 18. However, the average relative error for 5 testing samples is only 0.19. In other words, the predicted lives by the constructed model coincide well with the actual values. Thus, the constructed prediction model using GP can be used to well predict the life of tunnel structures.

3.1.2 Carbonation prediction model with four influential factors

By using the model considering four factors (the concrete cover thickness *c*, CO_2 concentration C_0, average temperature *T* and water-cement ratio *W*/*C*), the performance of GP to construct the complicated prediction model is verified.

In this study, the function set is $F=\{+,-,\times,\div,\text{power},\ln,\exp,\sin,\cos\}$, and the terminator set is $M=\{c,C_0,T,W/C\}$. The data samples in this study are shown in Table 4, which were randomly selected from Table 1. The training samples are the first 20 samples in Table 4, and the testing samples are the last 5.

Table 4 Data samples to construct the carbonation prediction model with four factors

Number	Average temperature	CO_2 concentration	Cover thickness	Water-cement ratio	Life
	T / °C	C_0	*c* / *mm*	*W*/*C*	T_{ri} / *year*
1	21.8	0.0633	50	0.4	75.91
2	24	0.0532	55	0.42	44.87
3	22.5	0.0538	55	0.4	115.97
4	18.67	0.1452	62	0.4	93.02
5	21.8	0.0673	50	0.56	34.98
6	12.5	0.0522	65	0.48	36.58
7	11.7	0.0738	60	0.52	37.52
8	1.2	0.048	60	0.46	94.09
9	22	0.048	50	0.32	114.92
10	0.3	0.0425	50	0.33	188.66
11	3.5	0.065	50	0.46	57.57
12	21	0.064	50	0.48	37.24
13	21.7	0.047	50	0.42	59.55
14	22	0.072	60	0.43	40.11
15	18.1	0.053	45	0.42	56.03
16	22.93	0.0926	50	0.39	97.01
17	16.7	0.134	50	0.5	46.16
18	16.2	0.077	50	0.48	53.35
19	15.2	0.071	45	0.46	31.06
20	13	0.057	45	0.5	61.04
21	14.5	0.073	55	0.46	37.51
22	15.4	0.078	45	0.4	76.45
23	21	0.081	50	0.42	44.08
24	22	0.077	50	0.4	70.19
25	18.3	1.022	45	0.42	71.87

To obtain the service life of the tunnel structure, the carbonation model that Uomoto Taketo (Pan 2005) proposed for reinforced concrete structures was used. For this model, four factors are considered: the concrete cover thickness, CO_2 concentration, average temperature and water-cement ratio. This model can be described as

$$t=\frac{c^2}{(k_{co_2}k_Tk_w)^2} \tag{6}$$

where $k_{co_2}=(2.804-0.847\lg C_0)\sqrt{C_0}$; $k_T=e^{8.748-\frac{2563}{T}}$; $k_w=2.94\frac{W}{C}-1.012$ or $k_w=2.39(\frac{W}{C})^2+0.446\frac{W}{C}-0.398$; *t* is the life; *c* is the concrete cover thickness; C_0 is the CO_2 concentration; *T* is the average temperature; *W*/*C* is the water-cement ratio.

The computing results by function (6) are shown in

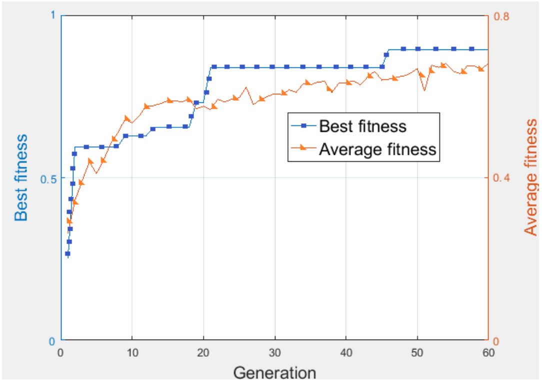

Fig. 8 Evolutionary process of the best fitness and average fitness for the carbonation prediction model with four factors

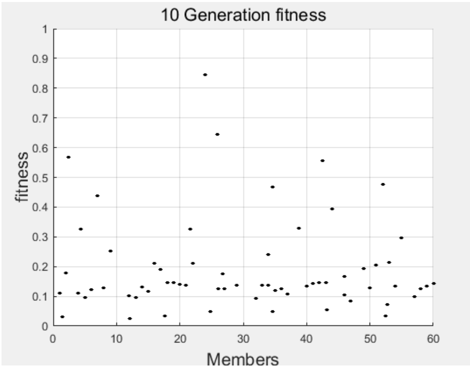

(a) 10 evolutionary generations

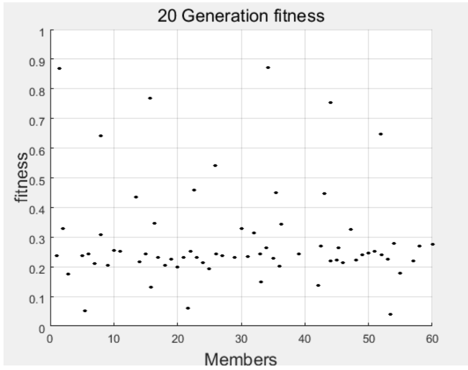

(b) 20 evolutionary generations

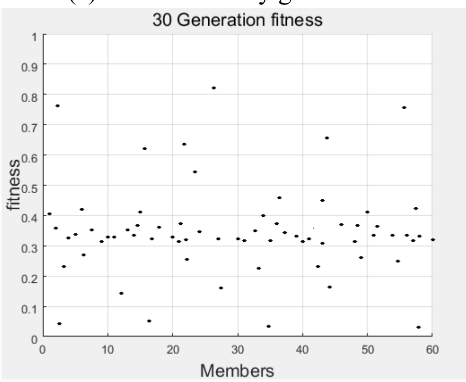

(c) 30 evolutionary generations

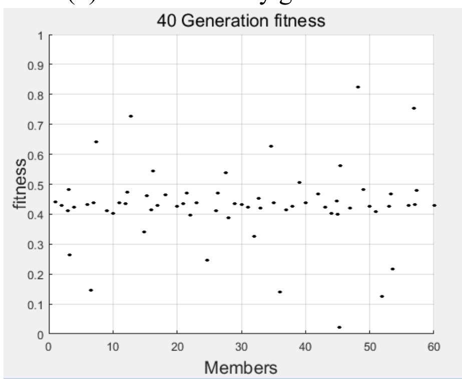

(d) 40 evolutionary generations

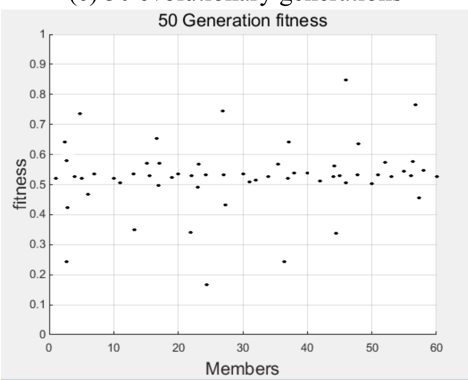

(e) 50 evolutionary generations

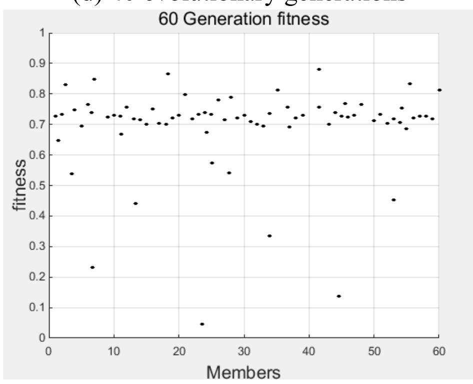

(f) 60 evolutionary generations

Fig. 9 Distribution of individual fitness for the carbonation prediction model with four factors

Table 4. Here, the computed life is also used as the real life. To determine the main parameters of GP, the method in section 3.1.1 was applied. The same parameters were used except the number of individuals, which is 60 here.

The data of training samples in Table 4 were used in the GP programmed by MATLAB, and the prediction model

Table 5 Comparison of the computed and real lives for the training samples by the carbonation prediction model with four factors

Number	Real life	Computing life	Absolute error	Relative error
1	75.91	82.60	6.69	0.0882
2	44.87	54.39	9.52	0.2122
3	115.97	107.58	8.39	0.0724
4	93.02	87.50	5.52	0.0593
5	34.98	25.30	9.68	0.2768
6	36.58	44.06	7.48	0.2045
7	37.52	28.55	8.96	0.2389
8	94.09	104.15	10.07	0.1070
9	114.92	123.19	8.27	0.0720
10	188.66	201.77	13.11	0.0695
11	57.57	51.46	6.11	0.1062
12	37.24	44.42	7.18	0.1928
13	59.55	55.05	4.49	0.0755
14	40.11	45.68	5.58	0.1390
15	56.03	49.60	6.42	0.1147
16	97.01	90.01	7.00	0.0722
17	46.16	38.52	7.64	0.1656
18	53.35	46.43	6.91	0.1296
19	31.06	20.39	10.68	0.3437
20	61.04	54.70	6.34	0.1038
Average value	—	—	7.80	0.14

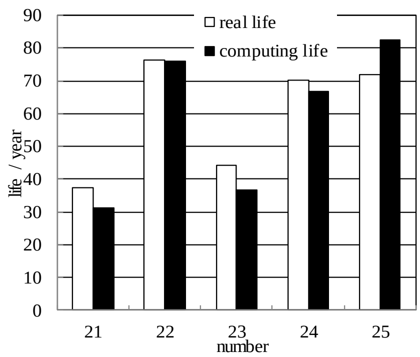

Fig. 10 Computing results of the testing samples by the carbonation prediction model with four factors

considering four factors can be obtained as

$$t=\frac{0.005}{c_0}\times\left(\frac{c}{(2.804-0.847\ln c_0)\times e^{8.784-\frac{2563}{T+293}}\times(2.94\frac{W}{C}-1.012)}\right)^2 \tag{7}$$

where t is the service life, and the other parameters can be found in the foregoing sections.

The evolutionary process of the best fitness and average fitness of one group is shown in Fig. 8. The distributions of individuals in the evolutionary process are shown in Fig. 9.

From Figs. 8 and 9, similar to Figs. 5 and 6, when the number of evolutionary generations increases, all values of the best fitness and average fitness gradually improve to a fixed one, and the individual fitness values in the population gradually congregate. In other words, the algorithm is also convergent, and the searching process of GP is satisfactory. Therefore, the GP can be used to model this complicated carbonation model with acceptable performance.

The computed and real lives of tunnel structures for the training samples are compared in Table 5.

From Table 5, the computing results for the training samples are consistent with the real lives, and the average relative error is only 0.14.

To verify the constructed model, the model was used to compute the lives of the testing samples. The computing results are shown in Fig. 10.

From Fig. 10, for 5 testing samples, all differences between the predicted lives by the constructed model and the real lives are small, and the average relative error for 5 testing samples is only 0.11. In other words, the predicted results by the constructed model are also consistent with the real ones, and the prediction ability of the GP model is satisfactory. Thus, GP can be used to construct the complicated prediction model for tunnel structures.

3.2 Engineering application (carbonation prediction model with multiple influential factors)

3.2.1 Carbonation prediction model by GP

From the above studies, GP can be used to construct the suitable carbonation prediction model only based on the data samples, regardless of how complicated the model is. Thus, in this study, based on the real data of engineering examples in Table 1, one prediction model that considers all twelve influence factors (CO_2 concentration C_0, average temperature T, relative humidity RH, water-cement ratio W/C, lining strength f, concrete cover thickness c, burial depth D, rock mass grading Q, clear width W, lining thickness L, carbonation remains x, design speed V) is constructed using GP.

In this study, the function set is also $F=\{+,-,\times,\div,\text{power},\ln,\exp,\sin,\cos\}$, and the terminator set is the set of twelve influence factors. The first 30 samples, i.e., the training samples, were used to construct the model, and the last ones were used to predict, i.e., testing samples. The method in section 3.1.1 was applied to determine the main parameters of GP. Thus, the identical parameters were used, except the number of individuals and maximum number for evolutionary generations are 100 and 200, respectively.

The training sample data in Table 1 were used in the GP programmed by MATLAB, and the prediction model that considers twelve factors can be obtained as

$$t=198.97\times\left|\frac{e^{\frac{x-15.297}{11.166}}-\dfrac{e^{\frac{C_0-0.0425}{0.1445}}}{\sin(\frac{T-0.3}{23.7})+\sin(\frac{\frac{W}{C}-0.28}{0.28})}}{\eta}\right|+32.91 \tag{8}$$

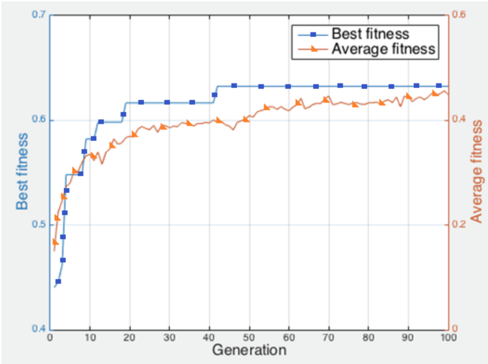

Fig. 11 Evolutionary process of the best fitness and average fitness for the carbonation prediction model with twelve factors

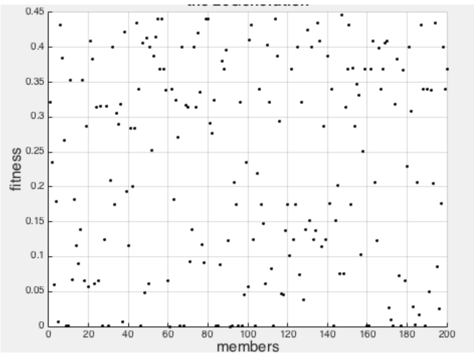

(a) 20 evolutionary generations

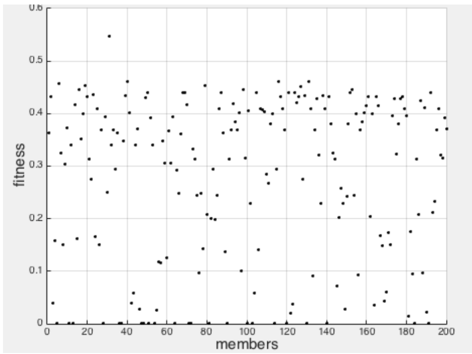

(b) 40 evolutionary generations

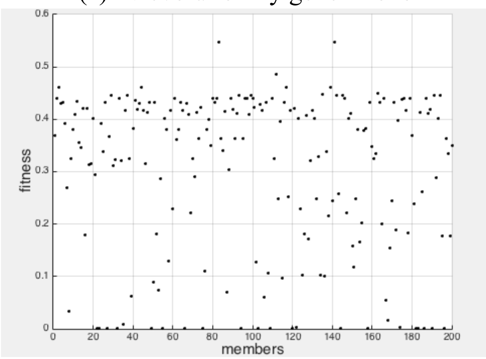

(c) 60 evolutionary generations

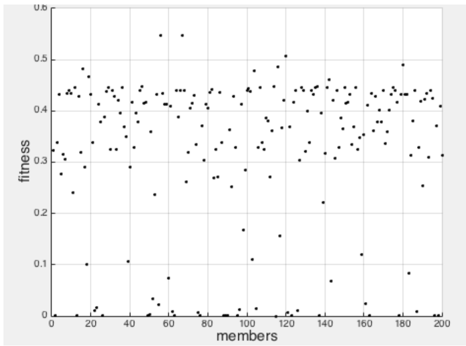

(d) 80 evolutionary generations

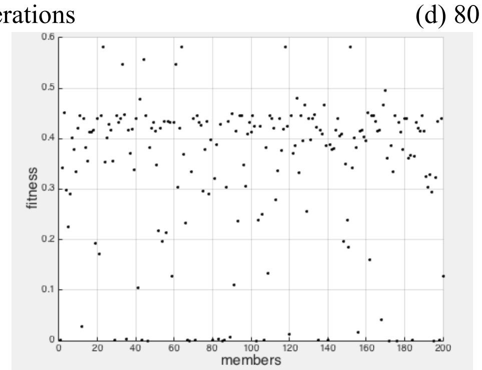

(e) 100 evolutionary generations

Fig. 12 Distribution of the individual fitness values for the carbonation prediction model with twelve factors

where

$$\eta = \sin(\frac{D-11}{1145}) \times \cos(\frac{W-3.75}{16.95}) + \cos(\frac{Q-3}{3}) - \ln(\frac{L-30}{35}) + \ln(\frac{f-16.7}{33.3}) + e^{\frac{RH-0.48}{0.37}} - \sin(\frac{V-30}{220}) + \ln(\frac{c-40}{25}) \quad (9)$$

t is the life, and the other parameters can be found in the foregoing sections.

The evolutionary process of the best fitness and average fitness is shown in Fig. 11.

From Fig. 11, the evolutionary process of the best

Table 6 Comparison of the computed and real lives of the training samples by the carbonation prediction model with twelve factors

Number	Real life	Computing life	Absolute error	Relative error
1	61.49	55.29	6.20	0.1009
2	66.51	74.34	7.83	0.1177
3	53.49	63.10	9.61	0.1797
4	36.81	44.26	7.45	0.2025
5	35.53	42.88	7.36	0.2071
6	43.80	51.80	8.00	0.1825
7	93.87	97.67	3.80	0.0405
8	40.63	53.91	13.28	0.3268
9	67.43	61.92	5.51	0.0818
10	231.88	211.22	20.66	0.0891
11	53.17	48.69	4.48	0.0842
12	52.85	50.14	2.71	0.0513
13	37.40	34.84	2.56	0.0684
14	48.01	42.29	5.72	0.1191
15	53.11	57.25	4.14	0.0780
16	54.34	67.85	13.51	0.2486
17	192.78	176.30	16.48	0.0855
18	50.21	45.67	4.54	0.0904
19	51.52	48.40	3.12	0.0606
20	56.08	61.82	5.74	0.1023
21	59.67	54.12	5.54	0.0929
22	32.91	41.20	8.30	0.2522
23	77.34	72.12	5.22	0.0675
24	57.96	54.87	3.09	0.0534
25	43.58	43.57	0.00	0.0001
26	44.33	44.61	0.28	0.0063
27	41.89	33.29	8.61	0.2055
28	42.88	43.10	0.23	0.0053
29	41.30	41.73	0.43	0.0105
30	39.28	49.83	10.54	0.2684
Average value	—	—	6.50	0.116

fitness stabilizes when the number of generations is approximately 50, and it quickly reaches stability. The average fitness is stable when the number of generations is approximately 60. Thus, the evolutionary process of GP for this model is quick and stable. To describe the evolutionary process of the entire population, the distributions of individuals during the evolutionary process are shown in Fig. 12.

In Fig. 12, the distributions of individuals in the population accumulate with the increase of the number for evolutionary generations. However, due to its complexity, this model has a poorer accumulating degree of population than the simple model, as shown in Figs. 6 and 9. Figs. 11 and 12 show that the stability of evolutionary process for this model is satisfactory.

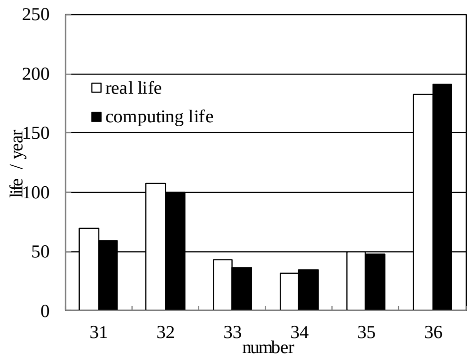

Fig. 13 Computed results of the testing samples by the carbonation prediction model with twelve factors

To verify the new prediction model, the training samples were computed by the new model. The computed and real lives of tunnel structures of the training samples are compared in Table 6.

In Table 6, the computed results by the new prediction model for 30 training samples are consistent with the real values, and the average relative error is only 0.116. Therefore, the approaching performance of the new prediction model is satisfactory.

To verify the prediction of the new model, the results of 6 testing samples are shown in Fig. 13. For comparison, the real lives are also shown in Fig. 13.

In Fig. 13, for 6 testing samples, all differences between the predicted lives by the constructed model and the real values are small, and the average relative error is only 0.09. Thus, the predicting results well coincide with the real ones, and the new model has acceptable prediction performance.

The above analyses show that GP can be used to construct the prediction model for tunnel structures only based on engineering samples, and the prediction ability of this model is satisfactory.

3.2.2 Comparison with the prediction model by artificial neural network

Because the artificial neural network (ANN) is the widely used method to construct the carbonation prediction model for reinforced concrete structures based on data analysis in previous studies, it is used to construct the carbonation prediction model for tunnel structures in this study. To validate the performance of the proposed method here, the prediction results by the ANN are compared with those by the GP method.

Based on experience and testing, the construction of ANN is determined as 12-24-1. The ANN was trained using the back-propagation algorithm. Its computing parameters are as follows: the iterating step is 0.15; the inertia parameter is 0.95; the termination error is 10^{-4}; the maximum iteration number is 1000. To improve the ANN model, here, the neuron activation function is the newly proposed Softplus function (Nair and Hinton 2010)

$$f(s) = \log(1+\exp(s)) \tag{10}$$

For comparison, similar to section 3.2.1 for the data samples, the first 30 samples are used as training samples to construct the prediction model. The last 6 samples are

Table 7 Computing results of the ANN model

Number	Real life	Computing life	Relative error
1	61.49	50.66	0.1761
2	66.51	75.25	0.1314
3	53.49	65.64	0.2271
4	36.81	51.3	0.3936
5	35.53	42.51	0.1964
6	43.80	56.62	0.2927
7	93.87	80.86	0.0853
8	40.63	50.75	0.2491
9	67.43	75.95	0.1263
10	231.88	187.89	0.1897
11	53.17	66.43	0.2118
12	52.85	44.67	0.1548
13	37.40	27.79	0.2569
14	48.01	40.57	0.1549
15	53.11	55.33	0.0418
16	54.34	69.72	0.283
17	192.78	171.8	0.1088
18	50.21	60.44	0.2037
19	51.52	46.9	0.0897
20	56.08	57.78	0.0303
21	59.67	64.32	0.0779
22	32.91	43.14	0.3108
23	77.34	70.65	0.0865
24	57.96	60.34	0.0411
25	43.58	50.46	0.1579
26	44.33	45.23	0.0203
27	41.89	37.57	0.1031
28	42.88	50.22	0.1712
29	41.30	43.5	0.0532
30	39.28	40.63	0.0344
31	46.56	54.28	0.2302
32	48.56	59.32	0.2834
33	79.40	85.46	0.1015
34	63.35	70.48	0.081
35	88.40	98.36	0.1918
36	217.91	186.84	0.1885

Table 8 Comparison of the computing results by the ANN and GP

Models	Results		
	Comparison items	Training samples	Testing samples
ANN	Average relative errors (%)	15.53	17.94
	Computing time (min)	4.57	0.73
GP	Average relative errors (%)	11.6	9.01
	Computing time (min)	2.21	0.01

testing samples, which are used to verify the model. The training samples are used to train the ANN, and the termination error for this ANN model is 0.0028. The results of ANN model for all 36 data samples are summarized in Table 7.

To compare the computing effect of two models (ANN and GP), the average relative errors of the training samples and testing samples of the two models are summarized in Table 8. For a fairer comparison, the computing efficiency and computing process time of two models are also compared in Table 8.

As shown in Table 8, GP has smaller average relative errors for the training samples and testing samples than the ANN, especially for the testing samples. Therefore, the GP model has better computing effect than the ANN model. The average relative error of the testing samples by GP is less than that of training samples. In contrast, the average relative error of the testing samples by ANN is larger than that of the training samples. Thus, GP has much better generalization prediction ability than ANN. Moreover, the computing time of the ANN model for the training samples is almost 4.57 minutes, and that for the testing samples is almost 0.73. However, the computing time of the GP model for the training samples is almost 2.21 minutes, and that for the testing samples is almost 0.01. Thus, the GP model has a much higher computing efficiency than the ANN model. Because the GP model using the training samples is an explicit mathematical expression, the computing speed for the testing samples is very fast. However, the ANN based model cannot be described by mathematical expressions, so this model has a much lower computing speed than the GP model. Considering the computing effect and efficiency comprehensively, the GP model is the preferred method to determine the suitable carbonation corrosion service life of tunnel structures. Moreover, because the prediction model constructed by the GP method is an explicit mathematical expression, the new method using GP can be simply and easily applied.

4. Discussion

For a typical evolutionary algorithm, some controlling parameters must be determined beforehand. These parameters seriously affect the performance of the prediction model based on GP. To provide guidance for the parameter determination, the effect of two main parameters on the performance of prediction model in section 3.2.1 is analyzed in detail: population size and sample size.

4.1 Population size

When the population size increases, the computing accuracy also increases, and the computing efficiency decreases. In other words, if the population size is small, the algorithm may quickly converge to a local extremum, and the computing result is very poor. In contrast, if the population size is large, the computational expense will seriously increase, and the computing efficiency is very low. Thus, the effect of the population size on the computing accuracy and efficiency is comprehensively

Table 9 Computing errors for different population sizes

Population size	Training samples		Testing samples	
M	Absolute error	Relative error	Absolute error	Relative error
20	14.38	0.2652	15.36	0.2944
40	9.13	0.1645	10.42	0.1832
80	3.99	0.0974	5.77	0.1047
120	2.07	0.0541	4.48	0.0693
180	1.17	0.0236	1.76	0.0304
240	0.94	0.0197	1.03	0.0236
480	0.76	0.0178	0.97	0.0199

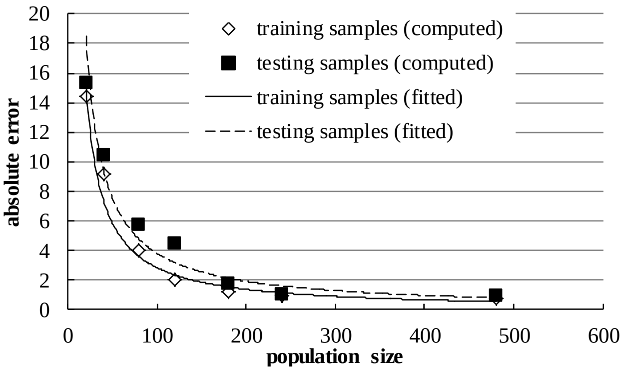

Fig. 14 Relationship of the absolute error and population size

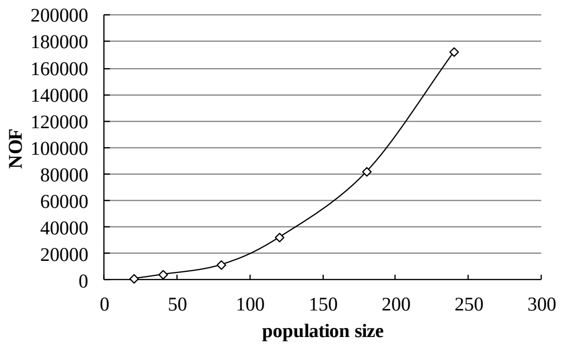

Fig. 15 Relationship of NOF and the population size

analyzed.

(1) Effect on the computing accuracy

Using different population sizes (20, 40, 80, 120, 180, 240, 480), the average computing errors of the training samples and testing samples are summarized in Table 9.

From Table 9, when the population size increases, the computing error decreases, and the decreasing extent reduces. For a thorough analysis, the relationship of the absolute errors for the training samples and testing samples with the population size is shown in Fig. 14.

Fig. 14 shows that all relationships between the absolute errors of training samples and testing samples and the population size are power functions. The fitting function for the training samples is

$$e_{train.p} = 341.12 \times M^{-1.04} \tag{11}$$

where $e_{train.p}$ is the errors of the training samples for different population size, and M is the population size.

The correlation coefficient of this function is 0.9636.

The fitting function for the testing samples is

$$e_{test.p} = 353.48 \times M^{-0.984} \tag{12}$$

where $e_{test.p}$ is the errors of the testing samples for different population size.

The correlation coefficient is 0.9357.

Therefore, the relationship between the computing accuracy and the population size is a power function, which should be

$$F = a \times M^{b} + c \tag{13}$$

where a, b and c are constants.

If the average values of parameters in fitting functions (11) and (12) are used, the three constants are: a=347.3; b=-1.012; c=0. Thus, the specific function for the relationship of the computing accuracy and population size can be obtained.

(2) Effect on the computing efficiency

To more suitably evaluate the computational efficiency of the algorithms with different population sizes (20, 40, 80, 120, 180, 240, 480), the number of objective function evaluations in the evolutionary process, which is denoted by NOF and represents the computational efficiency of the optimization algorithms (Gao 2016), is applied.

The relationship between NOF and the population size is shown in Fig. 15.

In Fig. 15, when the population size increases, NOF quickly increases. Their relationship is an exponential function, i.e., the increasing extent of NOF increases with the increase of population size. Moreover, when the population size exceeds 100, NOF sharply increases.

From the comprehensive analysis for the computing accuracy and computing efficiency, in this study, the optimal population size is determined as 100.

4.2 Sample size

The sample size seriously affects the evolutionary algorithm (Gao and Yin 2011, Ventura 2012). When the sample size increases, the computing results improve. However, it is very difficult to collect suitable engineering examples. In particular, for complicated carbonation problems for tunnel structures, it is almost impossible to collect many suitable engineering samples. Therefore, it is very important to suggest the minimal sample size. Because the sample size mainly affects the computing accuracy and slightly affects the computing efficiency (Gao and Yin 2011, Ventura 2012), only the effect on the computing accuracy is analyzed here.

Using different sample sizes (5, 10, 15, 20, 25, 30), the average computing errors of the training samples and testing samples are summarized in Table 10.

In Table 10, when the sample size increases, the computing error and decreasing extent decrease. For a thorough analysis, the relationship of the absolute errors for the training samples and testing samples and the sample size is shown in Fig. 16.

Fig. 16 shows that all relationships between the absolute errors of the training samples and testing samples and the

Table 10 Computing errors for different sample sizes

Sample size	Training samples		Testing samples	
S	Absolute error	Relative error	Absolute error	Relative error
5	18.44	0.4023	17.93	0.3947
10	13.44	0.2305	14.85	0.2589
15	8.79	0.1747	10.45	0.1595
20	7.83	0.1417	9.04	0.1203
25	6.62	0.1138	7.89	0.0987
30	6.53	0.0979	7.31	0.0937

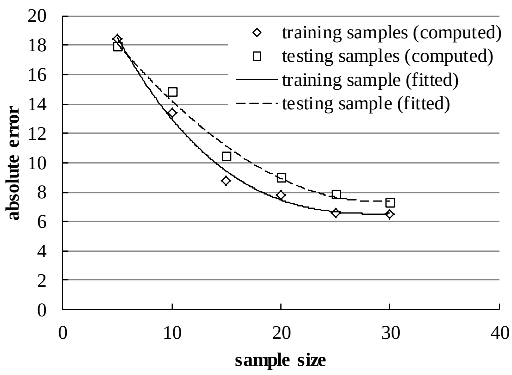

Fig. 16 Relationship of the absolute error and sample size

sample size are quadratic polynomial functions. The fitting function for the training samples is

$$e_{train.s} = 0.0584S^2 - 1.8883S + 36.617 \quad (14)$$

where $e_{train.s}$ is the errors of the training samples for different simple size, S is the sample size.

The correlation coefficient of this function is 0.9932.

The fitting function for the testing samples is

$$e_{test.s} = 0.0133S^2 - 0.9943S + 22.74 \quad (15)$$

where $e_{test.s}$ is the errors of the testing samples for different simple size.

Its correlation coefficient is 0.9892.

In Fig. 16, when the sample size is larger than approximately 20, all absolute errors for two samples slowly decrease; when it is larger than approximately 25, the absolute errors are almost unchanged. Therefore, the optimal sample size should be 25. However, considering the difficulty of collecting suitable engineering examples, in this study, we think that a sample size of 20 is acceptable.

5. Conclusions

As a main influence factor of the durability for underground structures, the carbonation-induced corrosion is studied here. It is very important to know that when structural damage due to reinforcement corrosion becomes visible, deterioration is usually in a late stage, and it may be too late to take any preventive or protection measures. Therefore, the service life prediction based on the corrosion damage of a structure is particularly important. For the complicated environment of underground structures, based on the data samples from real engineering examples of 36 tunnel engineering examples in China in carbonation environments, the intelligent method of genetic programming was used to construct the service life prediction model of tunnel structures. By which, the explicit expression of the carbonation prediction model of tunnel structures can be obtained. By using this model, for 30 training samples and 6 testing samples, the average relative errors are only 0.116 and 0.09, respectively. Moreover, for same data samples, the ANN based model has larger average relative errors for the training samples and testing samples (0.15 and 0.18) than the GP based one. And its computing times (4.57 minutes for the training samples and 0.73 minutes for the testing samples) are much longer than those by the new model (2.21 and 0.01 minutes). Therefore, GP can be used to construct the carbonation prediction model for tunnel structures only based on engineering samples, and the prediction ability of this model is satisfactory.

Moreover, the effect of two main controlling parameters on the performance of the constructed prediction model by genetic programming was analyzed in detail: the population size and sample size. The results show that the relationship between the computing accuracy and the population size is a power function, and the relationship between the computing efficiency and the population size is an exponential function. From the comprehensive analysis for the computing accuracy and computing efficiency, in this study, the optimal population size is determined to be 100. The relationship between the computing accuracy and the sample size is a quadratic polynomial function, and the optimal sample size should be 25 for this study.

Acknowledgments

The financial support from The Fundamental Research Funds for the Central Universities under Grant No. 2016B10214 is gratefully acknowledged.

References

Ahmad, S. (2003), “Reinforcement corrosion in concrete structures, its monitoring and service life prediction—a review”, *Cement Concrete Compos.*, **25**(4-5), 459-471. https://doi.org/10.1016/S0958-9465(02)00086-0.

Akpinar, P. and Uwanuakwa, I.D. (2016), “Intelligent prediction of concrete carbonation depth using neural networks”, *Bull. Transilvania Univ. Brasov*, **9**(58), 99-108.

Ann, K.Y., Pack, S.W., Hwang, J.P., Song, H.W. and Kim, S.H. (2010), “Service life prediction of a concrete bridge structure subjected to carbonation”, *Construct. Build. Mater.*, **24**(8), 1494-1501. https://doi.org/10.1016/j.conbuildmat.2010.01.023.

Bu, N.R., Yang, G.L. and Zhao, H. (2009), “Prediction of concrete carbonization depth based on DE-BP neural network”, *Proceedings of 2009 Workshop on Intelligent Information Technology Applications*, Nanchang, China, November.

Do, N.A., Oreste, P., Dias, D., Antonello, C., Irini, Djeran-Maigre, and Livio, L. (2014), “Stress and strain state in the segmental linings during mechanized tunnelling”, *Geomech. Eng.*, **7**(1), 75-85. https://doi.org/10.12989/gae.2014.7.1.075.

Do, N.A., Dias, D. and Oreste, P. (2018), “Numerical investigation of segmental Tunnel linings-comparison between the hyperstatic reaction method and a 3D numerical model", *Geomech. Eng.*, **14**(3), 293-299. https://doi.org/10.12989/gae.2018.14.3.293.

Feng, J.M. and Tian, M.Y. (2014), "A Study on the Classification and Grading of Environmental Effects on Tunnel Structure Durability", *Modern Tunnel Technol.*, **51**(3), 85-90 (in Chinese).

FIB (International Federation for Structural Concrete) (2009), *Structural Concrete: Textbook on Behaviour, Design and Performance*, FIB, Lausanne, Switzerland.

Gao, W. (2016), "Displacement back analysis for underground engineering based on immunized continuous ant colony optimization", *Eng. Optimiz.*, **48**(5), 868-882. https://doi.org/10.1080/0305215X.2015.1061814.

Gao, W. and Yin, Z.X. (2011), *Modern Intelligent Bionics Algorithm and Its Applications*, Science Press, Beijing, China (in Chinese).

Gokce, A., Koyama, F., Tsuchiya, M. and Gencoglu, T. (2009), "The challenges involved in concrete works of Marmaray immersed tunnel with service life beyond 100 years", *Tunn. Undergr. Sp. Technol.*, **24**(5), 592-601. https://doi.org/10.1016/j.tust.2009.01.001.

Jesus, R.M.D., Collado, J.A.M., Go, J.L., Rosanto, M.A. and Tan, J.L. (2017), "Modelling of carbonation of reinforced concrete structures in intramuros, Manila using artificial neural network", *Int. J. Geomate*, **13**(35), 87-92. https://doi.org/10.21660/2017.35.6683.

Kari, O.P., Puttonen, J. and Skantz, E. (2014), "Reactive transport modelling of long-term carbonation", *Cement Concrete Compos.*, **52**(8), 42-53. https://doi.org/10.1016/j.cemconcomp.2014.05.003.

Kellouche, Y., Boukhatem, B., Ghrici, M. and Tagnit-Hamou, A. (2019), "Exploring the major factors affecting fly-ash concrete carbonation using artificial neural network", *Neural Comput. Appl.*, **31**(S2), 969-988. https://doi.org/10.1007/s00521-017-3052-2.

Koza, J.R. (1992), *Genetic Programming: On the Programming of Computers by Means of Natural Selection*, MIT Press, Cambridge, U.S.A.

Lu, C.H. and Liu, R.G. (2009), "Predicting carbonation depth of prestressed concrete under different stress states using artificial neural network", *Adv. Artificial Neural Syst.*, 1-8. https://doi.org/10.1155/2009/193139.

Luo, D.M., Niu, D.T. and Dong, Z.P. (2014), "Application of Neural Network for Concrete Carbonation Depth Prediction", *Proceedings of the 4th International Conference on the Durability of Concrete Structures*, West Lafayette, Indiana, U.S.A., July.

Miranda, T., Dias, D., Pinheiro, M. and Eclaircy-Caudron, S. (2015), "Methodology for real-time adaptation of Tunnels support using the observational method", *Geomech. Eng.*, **8**(2), 153-171. https://doi.org/10.12989/gae.2015.8.2.153.

Nair, V. and Hinton, G.E. (2010), "Rectified linear units improve restricted Boltzmann machines", *Proceedings of 27th International Conference on Machine Learning*, Haifa, Israel, June.

Pan, H.K. (2005), "Durability and reliability of underground structure under carbonation environment", Ph.D. Dissertation, Tongji University, Shanghai, China (in Chinese).

Ranjith, A., Balaji Rao, K. and Manjunath, K. (2016), "Evaluating the effect of corrosion on service life prediction of RC structures-A parametric study", *Int. J. Sustain. Built Environ.*, **5**(2), 587-603. https://doi.org/10.1016/j.ijsbe.2016.07.001.

Spyridis, P. (2014), "Adjustment of tunnel lining service life through appropriate safety factors", *Tunn. Undergr. Sp. Technol.*, **40**, 324-332. https://doi.org/10.1016/j.tust.2013.10.006.

Sun, J. (2011), "Durability problems of lining structures for Xiamen Xiang'an subsea tunnel in China", *J. Rock Mech. Geotech. Eng.*, **3**(4), 289-301. https://doi.org/10.3724/sp.j.1235.2011.00289.

Taffese, W.Z., Al-Neshawy, F., Sistonen, E. and Ferreira, M. (2015), "Optimized neural network based carbonation prediction model", *Proceedings of the International Symposium Non-destructive Testing in Civil Engineering*, Berlin, Germany, September.

Taffese, W.Z. and Sistonen, E. (2013), "Service life prediction of repaired structures using concrete recasting method: State-of-the-art", *Procedia Eng.*, **57**, 1138-1144. https://doi.org/10.1016/j.proeng.2013.04.143.

Taffese, W.Z. and Sistonen, E. (2017), "Machine learning for durability and service-life assessment of reinforced concrete structures: Recent advances and future directions", *Automat. Construct.*, **77**, 1-14. https://doi.org/10.1016/j.autcon.2017.01.016.

Taffese, W.Z., Sistonen, E. and Puttonen, J. (2015), "Prediction of concrete carbonation depth using decision trees", *Proceedings of the 23rd European Symposium on Artificial Neural Networks, Computational Intelligence and Machine Learning*, Bruges, Belgium, April.

Ventura, S. (2012), *Genetic Programming - New Approaches and Successful Applications*, InTech, Rijeka, Croatia.

Woyciechowski, P.P. and Soko, J.J. (2017), "Self-terminated carbonation model as an useful support for durable concrete structure designing", *Struct. Eng. Mech.*, **63**(1), 55-64. https://doi.org/10.12989/sem.2017.63.1.055.

Xiang, R. (2009), "Prediction of concrete carbonation depth based on support vector regression", *Proceedings of the 2009 Workshop on Intelligent Information Technology Applications*, Los Alamitos, California, U.S.A., November.

Yuan, Y., Bai, Y. and Liu, J.H. (2012), "Assessment service state of tunnel structure", *Tunn. Undergr. Sp. Technol.*, **27**(1), 72-85. https://doi.org/10.1016/j.tust.2011.07.002.

Zeng, X.M., Wang, Z.Y., Fan, J.Q., Zhao, L., Lin, D.L. and Zhao, J. (2011), "Problems of durability and reinforcement measures for underground structures in China", *J. Rock Mech. Geotech. Eng.*, **3**(3), 250-259. https://doi.org/10.3724/SP.J.1235.2011.00250.

Zhang, J., Li, S.C., Li, L.P., Zhang, Q.Q., Xu, Z.H., Wu, J. and He, P. (2017), "Grouting effects evaluation of water-rich faults and its engineering application in Qingdao Jiaozhou Bay Subsea Tunnel, China", *Geomech. Eng.*, **12**(1), 35-52. https://doi.org/10.12989/gae.2017.12.1.035.

CC

Appendix (Reference for Table 1)

Chen, S.S. (2015), "A combination of rigidity and flexibility for leakage treatment of shabawan tunnel", *China Building Waterproofing*, (16), 15-18 (in Chinese).

Cheng, W.Y. (2006), "Research on parameters of initial support for phyllite stratum at Wushaoling Tunnel", *J. Railway Eng. Soc.*, (3), 37-39 (in Chinese).

Cheng, X.J. (2012), "Study on predicting the service life of highway tunnel lining structures", Ph.D. Dissertation, Southwest Jiaotong University, Chengdu, China (in Chinese).

Ding, H., Liu, R.Q., Hu J. Y. and Zheng, H. J. (2015), "Analysis of temperature field characteristics in the Jiangluling Tunnel", *Modern Tunn. Technol.*, **52**(1), 76-81 (in Chinese).

Dong, C.S., Zhang, X.X., Zhang, C. and Li, Y. (2015), "Test and research on freeze-thaw cycle of tunnel lining concrete in permafrost regions", *Highway*, (11), 244-247 (in Chinese).

Du, X.P., Liu, T., Li, D., Yuan, Y. and Li, T.S. (2006), "Evaluation and construction treatment of unfavorable geological section of Tiefengshan No.2 extra-long tunnel", *Highway Tunn.*, (4), 21-24 (in Chinese).

Du, X.P., Liu, T., Li, D., Yuan, Y. and Zhou, Y.S. (2006), "Evaluation and treatment of unfavorable geological condition segment in Tiefeng Tunnel", *Constr. Tech.*, **35**(7), 77-80 (in Chinese).

Feng, J.M. and Qiu, W.G. (2013), "Model test on effect of tunnel lining stiffness to structure durability", *J. Cent. South Univ. Sci. Tech.*, **44**(9), 3884-3890 (in Chinese).

Guo, Y. (2013), "Analysis on excavation disturbed zone of surrounding rock of Longwei Tunnel at Gui-Guang railway line for passengers", *Chin. J. Undergr. Sp. Eng.*, **9**(3), 615-619 (in Chinese).

Han, C.L. and Miu, H.F. (2000), "Introduction to Erlangshan Tunnel design", *Highway*, (12), 13-21 (in Chinese).

He, C.B., Cao, C.H. and Zhang, Z.B. (2014), "Construction technology of Huaying Mountain Tunnel under unfavorable geological conditions", *Railway Eng.*, (2), 63-66 (in Chinese).

Hou, J.Y., Yang, Q.X. and Guo C. (2015), "Study on comprehensive evaluation of operation safety of long highway tunnel", *Railway Standard Des.*, **59**(11), 88-91 (in Chinese).

Hu, J. (2008), "Qingling zhongnanshan highway tunnel large embedded depath monitoring measurement and numerical analysis ", Ph.D. Dissertation, Chang'an University, Xi'an, China (in Chinese).

Jiang, D.H. (2010), "Durability degradation law and life prediction of shield tunnel concrete segments", Ph.D. Dissertation, Nanjing University of Aeronautics and Astronautics, Nanjing, China (in Chinese).

Li, Q.F. (1988), "Discussion on hydrogeological conditions and regulation Ssheme of Wushaoling Tunnel on Lanxin Line", *J. Railway Eng. Soc.*, (1), 62-66 (in Chinese).

Li, S.C. (2012), "Construction techniques for the experimental section of the Taoshuping Tunnel in water-rich non-diagenetic fine sand", *Modern Tunn. Technol.*, **49**(4), 111-119 (in Chinese).

Li, S.C., Liu, Z.R. and Zheng, W.J. (2011), "Discussion on the construction techniques of Taoshuping Tunnel in immature fine sandstone stratum with rich water", *Modern Tunn. Technol.*,**48**(2), 120-124 (in Chinese).

Li, W.H. (2011), "Study on durability of lining structure of Foling tunnel", Ph.D. Dissertation, Beijing Jiaotong University, Beijing, China (in Chinese)

Li, X. and Qian, W.P. (2005), "Summary for the geological conditions of Wushaoling Tunnel", *Railway Investigation Survey.*, (4), 57-61 (in Chinese).

Liu, C. (2005), "Application of the high performance waterproof and corrosion prevention concrete in Wushaoling Tunnel", *Railway Standard Des.*, (9), 116-118 (in Chinese).

Liu, C.T. (2000), "Quality control of second lining construction of Erlangshan Tunnel", *Highway*, (12), 58-60 (in Chinese).

Liu, H. (2007), "Research on durability technology of long-span highway tunnel structure", Ph.D. Dissertation, Beijing Jiaotong University, Beijing, China (in Chinese).

Liu, J. (2014), "Research and discussion of clay hill tunnel risk assessment", *QingHai JiaoTong KeJi* , (5), 57-60 (in Chinese).

Liu, J.L., Yu, Q.H. and Xie, Y.T. (2010), "Structure of the tunnel lining durability forecast and control measures", *China Sci. Technol. Inform.*, (7), 76-79 (in Chinese).

Liu, T. (2010), "The study of structural damage & cause analysis of existed shield highway tunnel in soft soil area", *China Municipal Eng.*, (S1), 19-21 (in Chinese).

Liu, W. (2013), "Carbide and freeze-thaw effect on urban tunnel concrete lining structure durability research", Ph.D. Dissertation, Lanzhou University of Technology, Lanzhou, China (in Chinese).

Ma, J.Z. (2007), "Supporting technology for shallow rock excavation at the entrance of Taihangshan Tunnel", *J. Shijiazhuang Railway Inst.*, **19**(4), 122-126 (in Chinese).

Na, Q.C., Guo, H.Y., Hu, J.Y. and Cai, S. (2016), "Surrounding rock mechanical parameters test and back analysis of carbonaceous shale tunnel", *Chin. J. Undergr. Sp. Eng.*, (S2), 504-509 (in Chinese).

Nian, P.H. (2008), "Construction design of class III special surrounding rock of Gonghe Tunnel", *Railway Standard Des.*, (10), 81-87 (in Chinese).

Pan, X.F. (2012), "Design of special geological scheme for Xishan extra-long tunnel crossing construction prevention measures", *Highway*, (7), 316-321 (in Chinese).

Qian, H. (2011), "Surrounding rock stability and supporting structure performance in Foling Tunnel", *Transport Standard.*, (8), 48-51 (in Chinese).

Shi, Z.Y. (2009), "Rapid construction technology in water-rich phyllite stratum in Baojiashan Extra-long Tunnel", *Tunn. Constr.*, **29**(1), 72-75 (in Chinese).

Su, S. (2012), "Research on stability and support mechanical properties of fractured rock mass with different attitudes at Humaling Tunnel", *Subgrade Eng.*, (2), 95-98 (in Chinese).

Wang, B. and Li, G.L. (2003), "Quality control of secondary lining construction of Hegeshan Tunnel", *Southwest Highway*, (3), 59-60 (in Chinese).

Wang, L., Lin, G.J. and Chen, J.X. (2000), "Structure design of Huaying Mountain Tunnel", *East China Highway*, (2), 59-62 (in Chinese).

Wang, S.M., Yu, Q.Y., Peng, B., He, X.F. and Yao, J.B. (2016), "Three-dimensional discontinuous contact model for shield tunnels with double-layer lining based on plastic-damage model", *Chin. J. Rock Mech. Eng.*, **35**(2), 303-311 (in Chinese).

Yan, C.H., Sun, G.J., Wang, Y.T. and Yuan, X.B. (2017), "Analysis of regional spring basin characteristics and hydrological conditions of Southern Taihang Tunnel", *J. Railway Eng. Soc.*, **34**(1), 81-85 (in Chinese).

Yang, F.J., Wu, Y.P. and Han, C.H. (2008), "Finite element analysis of lining structure safety of Maijishan Tunnel", *Henan Building Mater.*, (8), 59-60 (in Chinese).

Yang, J.G., Liu, D.B., Wang, Q., Cao, H and Luo, D.S. (2012), "Reliability of the lining structure of the Majishan etra-long highway tunnel", *Modern Tunn. Technol.*, **49**(6), 77-80 (in Chinese).

Yang, L.D. and Gao, Z.X. (2003), "The durability for concrete lining structure of highway- tunnel and the thickness of concrete cover", *China Civ. Eng. J.*, **36**(12), 64-67 (in Chinese).

Yang, X., Yan, S.H. and Ma, L.N. (2012), "Analysis and prediction of temperature field of tunnels located in seasonal frozen area", *Tunn. Constr.*, **32**(1), 57-60 (in Chinese).

Yao, B.X. (2012), "Application of fly ash high performance concrete in Nanluliangshan Tunnel", *China Concrete*, (7), 89-91.

Yao, B.X. (2014), "Mix proportion design and construction control of durable concrete for extra-long tunnel", *Railway Eng.*, (1), 121-124 (in Chinese).

Yin, L.J. and Li, N.X. (2003), "Design of construction scheme for Wushaoling special long tunnel", *Chin. J. Rock Mech. Eng.*, **22** (S1), 2474-2477 (in Chinese).

Yuan, Z.X. (2013), "Study on hydrogeological conditions of south Lvliangshan Tunnel along the railway thoroughfare across Shanxi, Henan and Shandong", *Subgrade Eng.*, (4), 111-115 (in Chinese).

Zhang, J.S., Gao, S.Q., Liu, W., Ma, Q., Liu, D.W. and Hou, Z.Y. (2016), "Researches on long highway gas tunnel ventilation system based on ahp-fuzzy comprehensive method", *World Sci-Tech R & D*, (4), 778-782 (in Chinese).

Zhang, T. and Xia, R.H. (2010), "Research on techniques of TSP203Plus applied to the geological predication of long and large tunnels in Guiyang-Guangzhou PDL", *Chin. J. Eng. Geophys.*, **7**(5), 617-624 (in Chinese).

Zhao, G.Z., Tan, Z.S., Zeng, L. and Peng, G.F. (2007), "Durability experimental analysis of Longtoushan Tunnel lining structure", *Concrete*, (9), 107-109 (in Chinese).

Zhu, S. (2013), "Durability assessment and life prediction of tunnel's lining structure", Ph.D. Dissertation, Lanzhou University of Technology, Lanzhou, China (in Chinese).